Pentacoordinated chloro-iron(III) complexes with unsymmetrically substituted N2O2 quadridentate schiff-base ligands Syntheses, structures, magnetic and redox properties

J. Cisterna, V. Artigas, M. Fuentealba, P. Hamon, C. Manzur, J.-R. Hamon, D. Carrillo

inorganics

MDPI

Article

Pentacoordinated Chloro-Iron(III) Complexes with Unsymmetrically Substituted N_2O_2 Quadridentate Schiff-Base Ligands: Syntheses, Structures, Magnetic and Redox Properties

Jonathan Cisterna [1,†], Vania Artigas [1], Mauricio Fuentealba [1], Paul Hamon [2], Carolina Manzur [1], Jean-René Hamon [2,*] and David Carrillo [1,*]

[1] Laboratorio de Química Inorgánica y Laboratorio de Cristalografía, Instituto de Química, Facultad de Ciencias, Pontificia Universidad Católica de Valparaíso, Campus Curauma, Avenida Universidad 330, Valparaíso, Chile; jon.e.cisgar@gmail.com (J.C.); vania119@gmail.com (V.A.); mauricio.fuentealba@pucv.cl (M.F.); cecilia.manzur@pucv.cl (C.M.)

[2] CNRS, University Rennes, ISCR (Institut des Sciences Chimiques de Rennes)—UMR 6226, F-35000 Rennes, France; paul.hamon@univ-rennes1.fr

* Correspondence: jean-rene.hamon@univ-rennes1.fr (J.-R.H.); david.carrillo@pucv.cl (D.C.); Tel.: +33-223-235-958 (J.-R.H.); +56-322-274-914 (D.C.)

† Present address: Laboratorio de Química-Física, Departamento de Química, Universidad de Antofagasta: Campus Coloso, Avenida Universidad de Antofagasta 02800, Antofagasta, Chile.

Received: 19 November 2017; Accepted: 26 December 2017; Published: 29 December 2017

Abstract: Since their development in the 1930s, Schiff-base complexes have played an important role in the field of coordination chemistry. Here, we report the synthetic, spectral, structural, magnetic and electrochemical studies of two new pentacoordinated neutral chloro-iron(III) complexes (**3**,**5**) supported by dianionic $[N_2O_2]^{2-}$ tetradentate Schiff-base ligands unsymmetrically substituted by either a pair of acceptor (F and NO_2) or donor (ferrocenyl and OCH_3) groups. The electron-withdrawing Schiff-base proligand **2** and the complexes **3** and **5** were prepared in good yields (79–86%). Complex **3** was readily obtained upon reaction of **2** with anhydrous iron chloride under basic conditions, while the bimetallic derivative **5** was synthesized by condensation of the free amino group of the ferrocenyl-containing *O*,*N*,*N*-tridentate half-unit **4** with 5-methoxysalicylaldehyde in the presence of $FeCl_3$. The three new compounds were characterized by elemental analysis, FT-IR, UV–Vis, mass spectrometry and in the case of **2** by multinuclear NMR spectroscopy. The crystal structures of **3** and **5** revealed that in the two five-coordinate monomers, the iron atom showed distorted square-pyramidal geometry, with the N and O atoms of the Schiff-base ligand occupying the basal sites and the chlorine atom at the apex of the pyramid. Magnetic measurements showed a high-spin configuration (S = 5/2) for the Fe(III) ion in **3** and **5**. Reduction associated with the Fe(III)/Fe(II) redox couple occurred at −0.464 and −0.764 V vs. Ag/Ag^+, and oxidation taking place at the Schiff-base ligand was observed at 1.300 and 0.942 V vs. Ag/Ag^+ for **3** and **5**, respectively. A high-electronic delocalization of the Schiff-base ligand substituted by fluoro and nitro groups stabilizes the Fe(II) oxidation state and shifts the redox potential anodically.

Keywords: iron; unsymmetrically substituted tetradentate Schiff base; five-coordinate complex; square-pyramidal geometry; magnetism; crystal structure

1. Introduction

Since their first description by Hugo Schiff in 1864 [1], the so-called Schiff-base compounds have become, in their deprotonated form, one of the most widely used acyclic and macrocyclic

polydentate ligands in coordination chemistry [2–5]. Schiff-bases that have been characterized by an imine (>C=N–) or azomethine (–HC=N–) group are easily synthesized by straightforward condensation reactions of ketone or aldehyde with primary amines. *N*,*N*-bis(salicylidene)ethylenediamine H_2-salen, and *N*,*N*-bis(salicylidene)-*o*-phenylenediamine H_2-salphen, both reported for the first time by Pfeiffer and coworkers 85 years ago [6], probably represent the archetypical symmetric N_2O_2 tetradentate Schiff-base species. They were obtained by spontaneous condensation of salicylaldehyde with ethylenediamine and *o*-phenylenediamine, respectively, in a 2:1 stoichiometric ratio. In the early 1980s, Costes and coworkers described the first non-template synthesis of an unsymmetrically substituted N_2O_2 tetradentate Schiff-base through a two-step process [7]. First, 2,4-pentanedione was monocondensated with ethylenediamine to generate the parent *O*,*N*,*N*-tridentate half-unit. In a second step, reaction of the latter with salicylaldehyde formed the desired product in a 1:1:1 overall stoichiometric ratio. Owing to the easy tunability of their stereo-electronic structures and their flexible denticities, Schiff-base ligands readily form complexes with most of the transition metals that are stabilized in low as well as higher oxidation states and with various polyhedral arrangements [8,9]. As a consequence, this class of compounds has found utility in a number of fields from catalysis [10,11] to materials chemistry [12,13], including nonlinear optics (NLO) [14,15].

Besides their function as model compounds for biological systems [16], iron complexes of Schiff-base ligands are known to display interesting magnetic properties [17,18]. For instance, six-coordinate d^5 iron(III) complexes with N_3O_2X donor sets (X = S [19], Cl, N_3, NCO, NCS, NCSe, CN [20,21]) show spin-crossover activity. Striking thermochromic behavior in various organic solvents caused by spin-equilibrium has also been observed for ionic hexacoordinated iron(III) Schiff-base complexes [22]. On the other hand, neutral five-coordinate d^5 halogeno-iron(III) complexes containing planar tetradentate Schiff-base ligands show high-spin (HS) configuration (S = 5/2) and weak intermolecular antiferromagnetic exchange [17,22–24], presumably originating from pairwise interactions [25]. Moreover, some pentacoordinated [M(III)(salen)X] derivatives have also been found to be active NLO chromophores [26,27]. Recently, Karuppasamy et al. reported a series of eight chloro-iron(III) complexes with salen ligands symmetrically substituted with donor or acceptor groups prepared by a solvothermal one-pot method [28].

We have an ongoing interest in the synthesis and structural chemistry of new metal complexes featuring unsymmetrically substituted D-π-D′ and A-π-A′ Schiff-base ligands (D, D′, A, A′ denote donor and acceptor groups, respectively, and π a conjugated bridge), as building blocks to construct expanded D-π-A systems in order to enhance their second-order NLO responses. Recently we successfully prepared a series of robust neutral [M(salphen)]-type complexes (M = Ni, Cu) supported by dianionic $[N_2O_2]^{2-}$ tetradentate Schiff-base ligands (L^D, L^A) substituted by either a pair of donor or acceptor groups [29]. Encouraged by these results and continuing our efforts in this field we have now extended the scope to pentacoordinated chloro-iron(III) complexes of the type [Fe(L^D/L^A)Cl] as a preliminary study towards the elaboration of more complex coordination compounds. Interestingly, the labile chloro ligand is easily displaced by oxo anions [30], which allows the formation of iron(III) complexes bearing monodentate and bidentate anionic oxygen donor ligands [31]. Polynuclear species containing [Fe^{III}(L^D)] and [Fe^{III}(L^a)] units might be prepared using rigid aromatic linkers that have predetermined shapes and connectivities upon application of such a synthetic strategy. Herein we report the synthesis and full characterization of the new unsymmetrically substituted Schiff-base derivative **2** resulting from monocondensation of the half-units **1** with 5-nitrosalicylaldehyde and the A-π-A′ (**3**) and D-π-D′ (**5**) chloro-iron(III)-centered macroacyclic salphen-type Schiff-base complexes [Fe(N_2O_2)Cl] (see formulae in Schemes 1–3). Complex **3** is readily obtained upon reaction of **2** with anhydrous iron chloride in basic medium, whereas the homobimetallic compound **5** is formed by condensation of the free amino group of the organometallic half-units **4** with 5-methoxysalicylaldehyde in the presence of iron(III) salt. The three new compounds **2**, **3** and **5** were authenticated by X-ray diffraction studies. Redox and magnetic properties of the two iron(III) Schiff-base complexes were also investigated.

2. Results and Discussion

2.1. Syntheses

The acceptor unsymmetrically substituted Schiff base **2** was synthesized by the classical condensation reaction between half-unit (4-F–C_6H_4)–C(O)CH=C(CH_3)–N(H)–C_6H_4–NH_2 (**1**) [29] and 5-nitrosalicylaldehyde, in methanol at room temperature for 6 h (Scheme 1). Compound **2** was isolated as an air- and thermally stable yellow solid in good yield (79.7%). This proligand is soluble in the common organic solvents except diethyl ether and hydrocarbons.

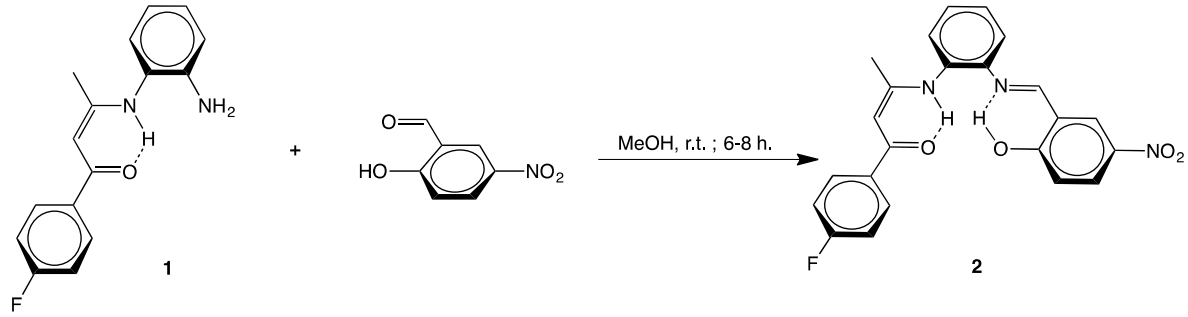

Scheme 1. Synthesis of the unsymmetrically substituted tetradentate Schiff base **2**.

The neutral mononuclear pentacoordinate chloro-iron(III) complex **3** was synthesized following a known one-pot two-step procedure [32]. First, the diprotic derivative **2** was doubly deprotonated with potassium *tert*-butoxide in THF at ambient temperature, before addition of a THF solution of anhydrous iron(III) chloride (Scheme 2). Complex **3** was isolated as a dark brown solid in excellent yield (86.4%).

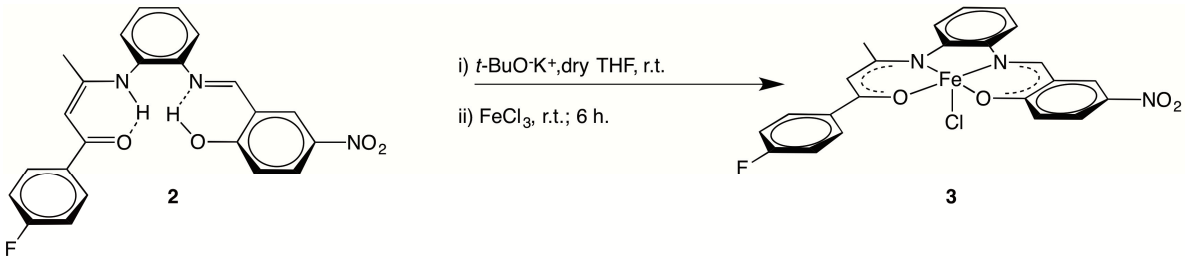

Scheme 2. Synthesis of the pentacoordinated chloro-iron(III) complex **3**.

As all attempts to synthesize and isolate the related electron-rich unsymmetrically substituted Schiff-base starting material were unsuccessful, the synthesis of the binuclear complex **5** was carried out via a previously used one-pot template methodology [29], that is, the condensation of the organometallic *ONN*-tridentate half-unit **4** [33] with 5-methoxy-2-hydroxibenzaldehyde in the presence of $FeCl_3$ (Scheme 3). Complex **5** was isolated as black needles in 79.1% yield.

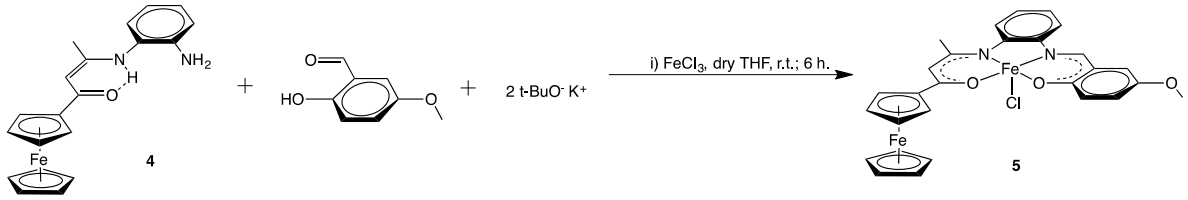

Scheme 3. Synthesis of the pentacoordinated chloro-iron(III) complex **5**.

Complexes **3** and **5** are air- and thermally stable and moisture insensitive on storage under ordinary conditions; they exhibit good solubility in common organic solvents but are insoluble in diethyl ether and aliphatic and aromatic hydrocarbons.

The composition and structures of the new compounds **2**, **3** and **5** were established by satisfactory elemental analyses, FT-IR, mass spectrometry, and multinuclear NMR spectroscopy in the case of **2**. In addition, the proligand **2** and the complexes **3** and **5** were authenticated by single-crystal X-ray diffraction studies (see Section 2.4). Observation of the molecular ion peaks (100% intensity) in the ESI^+ mass spectra of **2**, **3** and **5**, along with the good agreement of the experimental and simulated isotopic patterns, confirmed their structures.

2.2. FT-IR Spectroscopy

The solid-state FT-IR spectrum of the Schiff-base **2** exhibits two broad and weak bands at 3441 and 3070 cm^{-1} attributed to the ν(O–H) and ν(N–H) stretching vibrations, respectively. The shape and position of these bands are due to the two intramolecular N–H···O and O–H···N hydrogen bonds (see drawing of **2** in Scheme 1) [34,35]. Strong bands are also observed in the 1614–1584 cm^{-1} region and are attributed to the characteristic ν(C=N), ν(C=O) and ν(C=C) stretching modes of the Schiff-base skeleton. Likewise, two strong bands in the 1480–1340 cm^{-1} range have been assigned to the asymmetric and symmetric vibrational modes of the $–NO_2$ group [35,36]. The solid-state FT-IR spectra of the complexes **3** and **5** show a quite similar absorption band pattern (see Section 3.2), suggesting the analogy of their molecular structures. The disappearance of both the ν(O–H) and ν(N–H) absorption bands in the spectrum of complex **3** and the bathochromic shift by 8 cm^{-1} of the ν(C=N) stretching of the azomethine group upon complex formation [37,38] indicate that the acyclic $[N_2O_2]^{2-}$ ligand is bonded to the iron(III) ion in its dianionic form and in a tetradentate fashion through the N_2O_2-donor set of the Schiff-base ligand.

2.3. NMR Spectroscopy

The ^{1}H-NMR spectrum of the proligand **2**, recorded in CD_2Cl_2 at 298 K, displayed the expected resonance patterns consistent with the proposed structure (see Section 3.2 for complete assignments). The azomethine proton resonance was observed at 8.79 ppm, testifying the assembly of the expected acyclic Schiff base **2**. The amino and phenolic proton signals were seen at 13.05 and 13.71 ppm, respectively. Such deshielded resonances are in accordance with intramolecular hydrogen bonding of the amino proton with the carbonyl oxygen atom and of the hydroxyl proton with the imine nitrogen atom, thus closing, in both cases, a pseudo six-membered heterocycle (Scheme 1) [34,35,39,40]. The singlet resonance of the methine proton at 5.94 ppm testified the tautomeric keto-enamine form of **2**. The sharp singlet showing up at 2.09 ppm was ascribed to the methyl group. The four magnetically nonequivalent protons of the *o*-phenylene bridge gave rise to four different resonances of various multiplicities that were observed in the 8.41–7.02 ppm range, with the same integration ratio (see Section 3.2).

The ^{1}H-NMR findings were confirmed by the proton-decoupled ^{13}C-NMR spectral data with each type of carbon providing a separate resonance (see Section 3.2 for complete assignments). The enaminone structure was confirmed by the presence of the peak at 94.6 ppm, whereas the azomethine carbon resonated at 162.4 ppm. Owing to the intramolecular N–H···O hydrogen bonding, the carbonyl carbon resonance was upfield-shifted with respect to a pure ketonic carbon (>200 ppm) and found at 187.8 ppm. In the 4-fluorophenyl ring, the carbon atom directly bonded to the fluorine substituent appeared as a doublet with $^1J_{C,F}$ coupling constant of 252 Hz. The ortho and meta carbons appeared also as doublets with $^2J_{C,F}$ of 21 Hz and a $^3J_{C,F}$ of 9 Hz. By contrast, the fluorine nucleus appeared as a singlet at –110.15 ppm in the ^{19}F-NMR spectrum.

2.4. Crystal Structures

Good-quality single crystals for X-ray structure investigation were obtained for compounds **2**, **3** and **5**, either by slow evaporation of saturated dichloromethane solution in the cases of **2** and **3** or

by slow diffusion of diethyl ether into a saturated acetonitrile solution of **5**. The molecular structure of **2** is displayed in Figure 1, and those of **3** and **5** are depicted in Figure 2. Selected bond lengths and angles of **2** and of the [Fe(N_2O_2)Cl] coordination core of **3** and **5** are given in Tables 1 and 2, respectively, whereas other selected bond distances and angles of **3** and **5** are provided in Tables S1 and S2 of the Supplementary Materials, respectively. The Schiff-base proligand **2** crystallizes in the triclinic centrosymmetric space group $P\bar{1}$ with one molecule per asymmetric unit. Complexes **3** and **5** crystallize as solvated dichloromethane **3**·CH_2Cl_2 and acetonitrile **5**·0.5CH_3CN compounds, in the centrosymmetric space groups $P2_1/c$ and *Pbca*, respectively, with in each case one molecule in the asymmetric unit. The single-crystal X-ray diffraction studies confirm that each compound contains an unsymmetrically substituted electron-withdrawing or electron-releasing N_2O_2 salphen-type framework. The latter results from the monocondensation of half-unit **1** with 5-nitrosalicylaldehyde in the case of **2** and **3** and of the organometallic precursor **4** with 5-methoxysalicylaldehyde to form **5**. In **5**, the free cyclopentadienyl ring of the ferrocenyl substituent is disordered over two positions with an eclipsed/staggered occupancy ratio of 67/33 (Table S3, Supplementary Materials). For the sake of simplicity only the major conformer is taken into account in the discussion of the structure. As expected, the ferrocenyl unit features a typical linear η^5-Fe^{II}-η^5 sandwich structure [41], with almost parallel cyclopentadienyl rings and a ring centroid–Fe-ring centroid angle of 178.4°. The ring centroid-iron distances are of 1.674 and 1.636 Å for the free and substituted rings, respectively. The structures of **2** and **3** are stabilized by networks of intra- and intermolecular hydrogen bonds that connect the neighboring entities (Figures S1 and S2, Supplementary Materials).

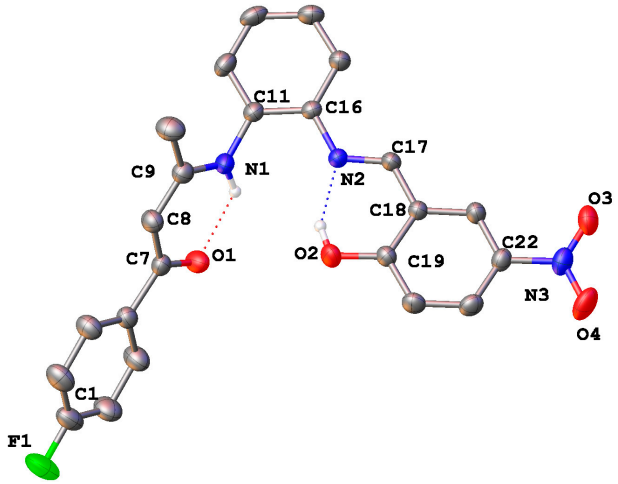

Figure 1. Molecular structure of the Schiff-base proligand **2** showing partial atom numbering scheme. Nonrelevant hydrogen atoms are omitted for clarity. Thermal ellipsoids are drawn at 50% probability.

The potentially tetradentate acyclic ligand **2** exists as the Z-*s*-Z conformational form [34,35] in the enaminone part of the molecule (Figure 1) whose plane is almost coplanar with that of the 4-fluorophenyl substituent, making a dihedral angle of 6.3(1)°. The structure also reveals two intramolecular hydrogen bonds that close two pseudo-six-membered rings through the resonant ···O=C–C=C–NH··· fragment [42], with alternating double, single, double and single bonds between the vicinal O, C and N sp^2-hybridized atoms (Table 1). The first hydrogen bond is located between the amino hydrogen atom and the carbonyl oxygen atom, whereas the second one takes place between the hydroxo substituent of the salicylidene ring and the imine nitrogen, with N···O separations of 2.638(2) and 2.586(2) Å, respectively (Table S4, Supplementary Materials). Lastly, the enaminone and salicylaldimine planes rotate by 69.0(1)° and 9.8(1)°, respectively, with respect to that of the *o*-diazophenylene spacer, while the nitro group is virtually coplanar with the salicylidene ring with a dihedral angle of 2.7(4)°.

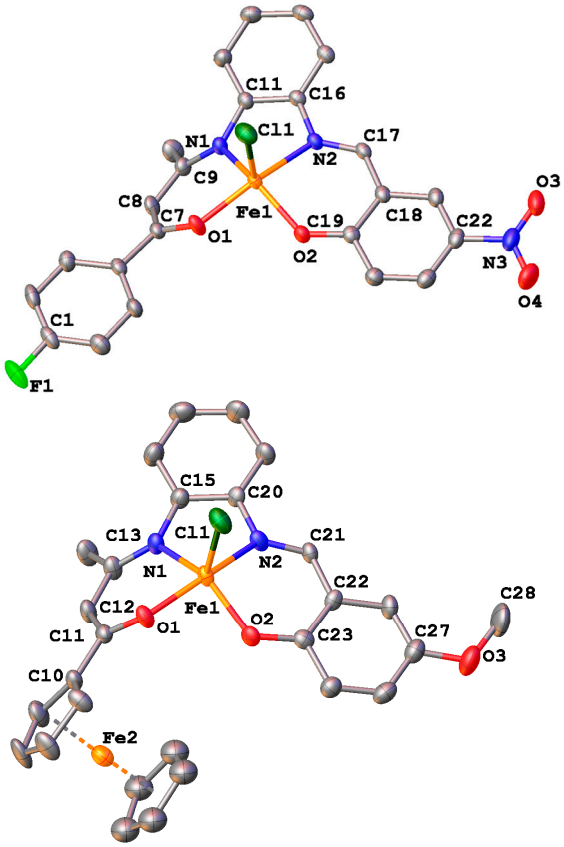

Figure 2. Molecular structures of **3**·CH_2Cl_2 (**top**) and **5**·0.5CH_3CN (**bottom**) with partial atom labelling schemes. Hydrogen atoms and crystallization solvent molecules have been omitted for clarity. Thermal ellipsoids are drawn at 50% probability.

Table 1. Selected bond distances (Å) and angles (°) for compound **2**.

Bond Distances			
O(1)–C(7)	1.249(2)	O(2)–C(19)	1.329(2)
N(1)–C(9)	1.333(3)	N(2)–C(17)	1.279(2)
C(7)–C(8)	1.421(3)	C(17)–C(18)	1.444(3)
C(8)–C(9)	1.373(3)	C(18)–C(19)	1.413(3)
N(1)–C(11)	1.428(2)	N(2)–C(16)	1.415(2)
F(1)–C(1)	1.3250(17)	N(3)–C(22)	1.460(3)
N(3)–O(3)	1.220(3)	N(3)–O(4)	1.217(3)
Bond Angles			
O(1)–C(7)–C(8)	122.18(19)	O(2)–C(19)–C(18)	121.10(17)
C(7)–C(8)–C(9)	124.1(2)	C(17)–C(18)–C(19)	121.29(17)
N(1)–C(9)–C(8)	121.21(19)	N(2)–C(17)–C(18)	121.80(17)
C(9)–N(1)–C(11)	126.32(18)	C(16)–N(2)–C(17)	121.95(16)
O(3)–N(3)–O(4)	123.3(2)	O(3)–N(3)–C(22)	118.33(18)

The principal structural features of complexes **3** and **5** are depicted in Figure 2. The two structures consist of discrete molecules of [Fe(L^A/L^D)Cl]. In each compound, the iron(III) ion occupies the central position of a distorted pentahedral arrangement. Out of its five coordination sites, four positions are occupied by the dianionic tetradentate Schiff-base ligand through two nitrogen (amino and imino) atoms and two oxygen (carbonyl and phenoxido) atoms. The remaining fifth coordination is satisfied by a chloro ligand. The trigonality index (τ) [43] that is a parameter of distortion from the

square-pyramidal to the trigonal-bipyramidal geometry has been calculated for the two pentahedral iron sites. The τ values are found to be 0.32 and 0.45 for **3** and **5**, respectively, indicating that the pentacoordinated environment is strongly distorted from a perfectly square pyramid (τ = 0). The iron atoms are, indeed, substantially protruded from the ligand plane, which represents the typical five-coordinate square-pyramidal arrangement. These iron atoms are displaced by 0.529 and 0.576 Å in **3** and **5**, respectively, from the least-squares plane defined by the Schiff-base donor atoms. This reflects the strain exerted by the ligand structure and results in a significantly bent arrangement of the ligand that is reflected in the angles of 39.7(2)° and 52.0(4)°, respectively, between the two planes of the [O–C–C–C–N] chelate rings of the ligands. The transoid O(1)–Fe–N(2) angles were found at slightly below 160° (Table 2), whereas the O(2)–Fe–N(1) angles are of 138.13(13)° and 132.3(3)° in **3** and **5**, respectively. The O–Fe–O angle averages to 92.8° (Table 2).

Table 2. Selected bond distances (Å) and angles (°) within the first [Fe(N_2O_2)Cl] coordination sphere for compounds **3**·CH_2Cl_2 and **5**·0.5CH_3CN.

	3·CH_2Cl_2	**5·0.5CH_3CN**
Bond Distances		
Fe(1)–O(1)	1.918(3)	1.925(6)
Fe (1)–O(2)	1.900(3)	1.877(7)
Fe (1)–N(1)	2.063(3)	2.068(8)
Fe (1)–N(2)	2.109(3)	2.060(7)
Fe (1)–Cl(1)	2.208(12)	2.229(3)
Bond Angles		
O(1)–Fe(1)–N(2)	157.26(13)	159.5(3)
O(2)–Fe(1)–N(1)	138.13(13)	132.3(3)
O(1)–Fe(1)–O(2)	93.21(12)	92.4(3)
O(1)–Fe(1)–N(1)	88.31(12)	87.6(3)
O(2)–Fe(1)–N(2)	86.69(12)	87.7(3)
N(1)–Fe(1)–N(2)	76.92(12)	77.7(3)
O(1)–Fe(1)–Cl(1)	101.80(10)	101.4(2)
O(2)–Fe(1)–Cl(1)	110.17(10)	112.9(2)
N(1)–Fe(1)–Cl(1)	110.41(10)	113.7(2)
N(2)–Fe(1)–Cl(1)	99.55(9)	97.4(2)

The Fe–O, Fe–N and Fe–Cl bond lengths are almost identical in the two molecules (Table 2), and are consistent with the corresponding values measured in similar pentacoordinated iron(III)-chloride complexes supported by the N_2O_2 tetradentate Schiff-base ligand [17,24,25,44–49]. The average values are 1.921 and 1.888 Å (Fe–O), 2.064 and 2.084 Å (Fe–N), and 2.218 Å (Fe–Cl). Studies of metal complexes with tetradentate Schiff-base ligands have shown that the iron-to-imine nitrogen bond distance is an indicator of the electronic spin state of the metal ion [24,49,50]. The Fe–N bond lengths are in the range 1.93–1.96 Å for the low-spin state and in the range 2.00–2.10 Å for the high-spin configuration. In the structures of **3** and **5** reported here, the Fe–N bond distances of 2.109(3) and 2.060(7) Å, respectively, clearly suggest that the iron(III) ion in both complexes is in the high-spin state. This is consistent with the results of the magnetic measurements (see Section 2.7).

On the other hand, the [O(1)–CCC–N(1)] plane makes dihedral angles of 34.8(2)° and 14.8(5)° with that of its 4-fluorophenyl and substituted Cp ring substituents in **3** and **5**, respectively. Like in the free proligand **2**, the NO_2 group is almost coplanar (4.1(6)°) with the salicylidene ring in **3**.

2.5. Electronic Absorption Spectra

The UV-Vis spectra of the five-coordinate Schiff-base complexes **3** and **5** were recorded in CH_2Cl_2 (ε_r = 8.90) and in DMSO (ε_r = 47.6). The deconvoluted spectral data are gathered in Table 3, whereas both experimental and deconvoluted spectra are displayed in Figure 3 (for those recorded in CH_2Cl_2)

and Figure S3 (for those recorded in DMSO). A strong broad absorption band was observed in the 300–430 nm range, whereas a set of two to three absorption bands appeared in the 450–650 nm range. The high-energy bands are attributed to π–π* intra-ligand charge-transfer transitions (ILCT), and the lower-energy bands are assumed to involve ligand-to-metal and metal-to-ligand charge-transfer transitions in a lesser extent [27]. In the spectrum of **5** recorded in DMSO (Figure S3), the band at 502 nm could be indicative of high-spin species, while the lowest energy band observed around 650 nm could arise from d–d transitions [22].

Table 3. Deconvoluted UV-Vis absorption data for complexes **3** and **5**.

Comp.	λ/nm (log ε) CH_2Cl_2	λ/nm (log ε) DMSO	Δ*E* (cm^{-1})
3	301 (4.42)	311(4.38)	+1068
	349(4.22)	357(3.04)	+642
	387(4.08)	383(3.79)	−270
	446(3.51)	420(4.12)	−1388
	453(3.20)	466(3.22)	+616
5	292(4.22)	303(4.47)	+1243
	375(3.90)	392(4.34)	+1156
	435(3.95)	447(3.54)	+617
	476(4.35)	475(3.76)	−44
	-	502(3.48)	-
	-	653(3.00)	-

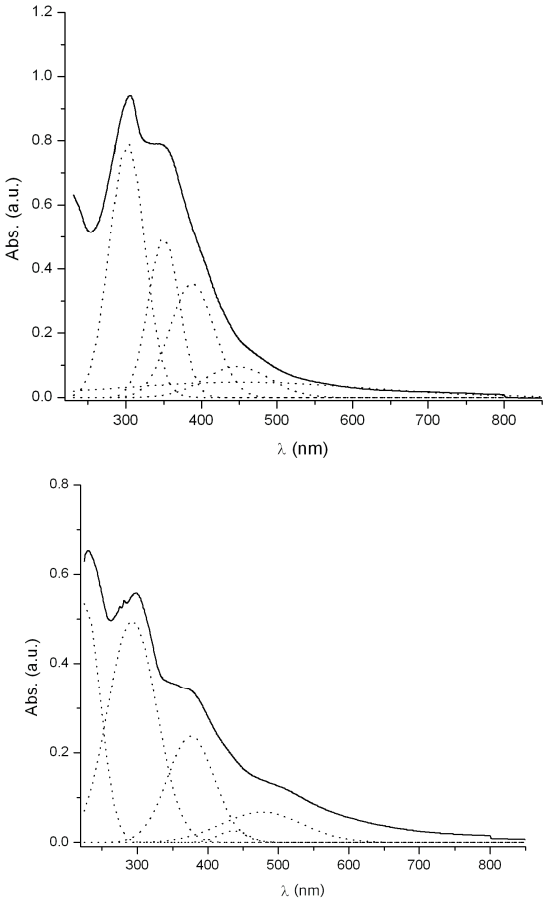

Figure 3. Experimental UV-Vis spectra of complexes **3** (**top**, full line) and **5** (**bottom**, full line) recorded in CH_2Cl_2 at 20 °C, and their respective deconvoluted spectra (dotted lines).

On moving from the less polar solvent to the more polar one, the two compounds exhibit solvatochromism, that is, their maximal absorption peaks show hypsochromic or bathochromic shifts (see Table 3). This indicates the change of dipole moments in the ground and excited states, verifying the existence of intramolecular charge transfer and suggestive of molecular first hyperpolarizabilities with nonzero values [27].

2.6. Electrochemical Properties

Cyclic voltammetry (CV) was used to investigate the redox properties of the two five-coordinate chloro-iron(III) Schiff-base complexes **3** and **5** (Figure 4). The measurements were carried out in methylene chloride solution containing 0.1 M nBu$_4$N$^+$PF$_6^-$ as supporting electrolyte, at 293 K in the +1.5 to −1.0 V potential range, with redox potentials quoted against Ag/Ag$^+$ reference electrode. The CV of **3** exhibited a reversible redox process centered at −0.454 V (ΔE_p = 92 mV, i_{pc}/i_{pa} = 1.10). This slight discrepancy from an idealized chemical reversibility (i_{pc}/i_{pa} = 1.00) could be accounted for by the fact that the electrogenerated iron(II) species is excessively air sensitive, leading to the formation of the thermodynamically stable μ-oxo bridged dimer [(L)Fe–O–Fe(L)] [51]. The CV of the more electron-rich derivative **5** showed an irreversible reduction wave at a more cathodic potential (E_{pc} = −0.764 V). These redox events have been assigned to the Fe(III)/Fe(II) couple [28,52]. Both compounds also underwent oxidative processes taking place at the Schiff-base ligands: an irreversible oxidation wave at E_{pa} = 1.300 V in the case of **3**, and a quasi-reversible one centered at 0.942 V (ΔE_p = 115 mV, i_{pc}/i_{pa} = 0.99) in the case of **5**. This electrochemical behavior is reminiscent of that observed with [Fe(salen)Cl] derivatives possessing either symmetrically [28] or unsymmetrically substituted N_2O_2 tetradentate Schiff-base ligands [52]. Here, the observed opposite redox behavior between **3** and **5** is in accordance with the electronic donor/acceptor ability of the two ligands as previously observed in the Ni(II) and Cu(II) series [29]. On the other hand, the CV of the homobimetallic complex **5** also presents a quasi-reversible redox process at 0.333 V (ΔE_p = 118 mV, i_{pc}/i_{pa} = 0.85) attributed to the monoelectronic oxidation of the ferrocenyl fragment that is anodically shifted by ~160 mV with respect to free ferrocene under the same experimental conditions. This anodic shift is presumably due to the electron-withdrawing ability of the Schiff-base chloro-iron(III) unit. In fact, we previously found such a large anodic shift (168 mV) in the case of a Cu(II) complex with a ferrocenyl-containing Schiff-base ligand bearing a nitro substituent [36]. Lastly, the shoulders at 0.500 and 0.460 V observed at v = 0.1 V/s disappear at higher scan rates, suggesting some adsorption/desorption process at the vitreous carbon working electrode.

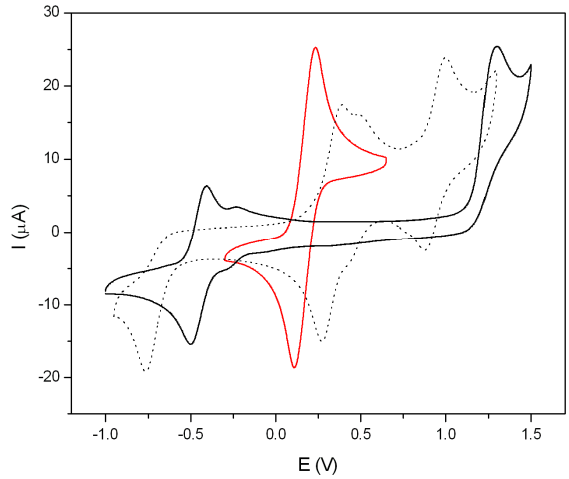

Figure 4. Cyclic voltammograms of **3** (black line) and **5** (dotted line), recorded in CH_2Cl_2 containing 0.1 M n-Bu$_4$N$^+$PF$_6^-$ at a vitreous carbon working electrode at 293 K, v = 100 mV·s^{-1}, reference electrode Ag/Ag$^+$, internal reference ferricenium/ferrocene redox couple (red line).

2.7. Magnetic Measurements

The room temperature value of $\chi_M T$, with χ_M the molar magnetic susceptibility and T the temperature in Kelvin, is equal to 4.2 and 4.1 $cm^3 \cdot K \cdot mol^{-1}$ for **3** and **5**, respectively. These values are fully compatible with a Fe(III) high-spin complex (the expected value is 4.375 $cm^3 \cdot K \cdot mol^{-1}$ with a Zeeman factor equal to 2.00). $\chi_M T$s remain quasi-constant on cooling down to 50 K (Figure 5). Below this temperature, $\chi_M T$s abruptly decrease, which can be the sign of the presence of antiferromagnetic interaction between magnetic centers (see here below) [22–25].

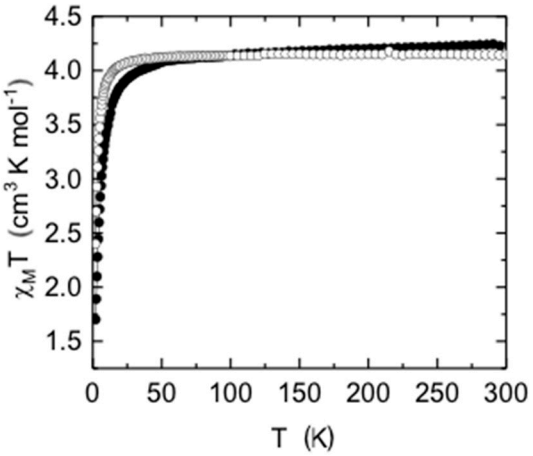

Figure 5. Thermal variation of $\chi_M T$ between 2 and 300 K for **3** (full circles) and **5** (empty circles).

3. Materials and Methods

All manipulations were performed under dry nitrogen atmosphere using standard Schlenk techniques. Solvents were dried and distilled according to standard procedures [53]. 5-nitrosalicylaldehyde, 5-methoxy-2-hydroxybenzaldehyde, iron (III) chloride and potassium *tert*-butoxide were purchased from Aldrich (Sigma-Aldrich Co., St. Louis, MO, USA) and used without further purification. Half units (4-F–C_6H_4)–C(O)CH=$C(CH_3)$N(H)-*o*-$C_6H_4NH_2$ (**1**) [29] and {(η^5-C_5H_5)Fe(η^5-C_5H_4)–C(O)CH=$C(CH_3)$N(H)-*o*-$C_6H_4NH_2$ (**4**) [33] were synthesized according to published procedures, characterized by FT-IR and ^{1}H-NMR spectroscopy and checked against literature data.

Solid-state FT-IR spectra were recorded on a Perkin-Elmer Model 1600 FT-IR spectrophotometer (Perkin-Elmer Inc., Waltham, MA, USA) with KBr disks in the 4000 to 450 cm^{-1} range, electronic spectra on a Shimadzu UV-1800 spectrophotometer (Shimadzu Co., Kioto, Japan), and NMR spectra on a Bruker Avance III 400 spectrometer (Bruker Co., Billerica, MA, USA) at 298 K. All NMR spectra are reported in parts per million (ppm) relative to tetramethylsilane (Me_4Si) for ^{1}H- and ^{13}C-NMR spectra, with the residual solvent proton and carbon resonances used as internal standards. Chemical shifts of ^{19}F-NMR spectra are referenced against external $CFCl_3$. All signals have been assigned using their appropriate chemical shift (δ in ppm), multiplicity, coupling constants (*J* in Hertz), and integral ratio. The following abbreviations apply for signal multiplicity of peaks within spectra: s = singlet, d = doublet, t = triplet, m = multiplet, br = broad. High-resolution electrospray ionization mass spectra (ESI-MS) were conducted on a Bruker MAXI 4G mass spectrometer in positive mode, at the Centre Régional de Mesures Physiques de l'Ouest (CRMPO, Université de Rennes 1, France). Elemental analyses were carried out on a Thermo-Finnigan Flash EA 1112 CHNS/O analyzer by the Microanalytical Service of the CRMPO. Cyclic voltammetry (CV) measurements were performed using a CH Instruments model Ch604E potentiostat (Ch Instruments Inc., Austin, TX, USA), using a standard three-electrode setup with a vitreous carbon working electrode, platinum wire auxiliary electrode, and Ag/Ag^+ as the reference electrode. Dichloromethane solutions were 1.0 mM in the compound under study and 0.1 M in the supporting electrolyte *n*-$Bu_4N^+PF_6^-$ with voltage scan rate of

100 mV·s^{-1}. The ferricenium/ferrocene redox couple was used as internal reference for the potential measurements. The temperature dependences of the magnetizations for powdered samples have been measured with a SQUID magnetometer (Quantum design MPMS-XL5; Quantum design Inc., San Diego, CA, USA) operating between 2 and 300 K at a constant field of 2 kOe below 20 K and 10 kOe above. The experimental data have been corrected from the sample holder diamagnetism and the intrinsic diamagnetism estimated from the Pascal's tables [54]. Melting points were determined in evacuated capillaries on a Kofler Bristoline melting point apparatus and were not corrected.

3.1. X-ray Crystal Structure Determination Measurements

Single crystals of **2**, **3**·CH_2Cl_2 and **5**·0.5CH_3CN were grown as depicted in Section 2.4. A well-shaped crystal of each compound was mounted on top of glass fibers in a random orientation. Intensity diffraction data were collected at 296 K on a Bruker D8 QUEST diffractometer (Bruker Co., Billerica, MA, USA) equipped with a bidimensional CMOS Photon100 detector (Bruker Co., Billerica, MA, USA), using graphite monochromated Mo Kα radiation (λ = 0.71073 Å). The diffraction frames were integrated using the APEX2 package, and were corrected for absorptions with SADABS. The structures of **2** and **5**·0.5CH_3CN were solved using OLEX2 [55], with the *SHELXS* structure solution program using Direct Methods [56]. The structure of **3**·CH_2Cl_2 was solved by Patterson methods [57]. The structures of **2** and **5**·0.5CH_3CN were refined with CGLS minimisation and that of **3**·CH_2Cl_2 with full-matrix least-squares methods based on F^2 (*SHELXL*-97) [56,57]. For the three compounds, non-hydrogen atoms were refined with anisotropic displacement parameters. All hydrogen atoms were included in their calculated positions, assigned fixed isotropic thermal parameters and constrained to ride on their parent atoms. A summary of the details about crystal data, collection parameters and refinement are documented in Table 4, and additional crystallographic details are in the CIF files. ORTEP views were drawn using OLEX2 software [55].

Table 4. Crystal data, details of data collection and structure refinement parameters for compounds **2**, **3**·CH_2Cl_2 and **5**·0.5CH_3CN.

	2	**3·CH_2Cl_2**	**5·0.5CH_3CN**
Empirical Formula	$C_{23}H_{18}FN_3O_4$	$C_{23}H_{16}ClFFeN_3O_4 \cdot CH_2Cl_2$	$C_{28}H_{24}ClFe_2N_2O_3 \cdot 0.5C_2H_3N$
Formula mass, g·mol^{-1}	419.40	593.61	604.17
Collection T, K	296	296	296
Crystal system	triclinic	monoclinic	orthorhombic
Space group	$P\bar{1}$	$P2_1/c$	*Pbca*
a (Å)	6.50650(10)	13.7047(8)	17.1576(10)
b (Å)	8.9928(2)	7.3909(5)	13.8793(10)
c (Å)	17.7353(5)	24.6860(14)	23.1768(17)
α (°)	98.3710(11)	90	90
β (°)	92.8731(11)	99.469(2)	90
γ (°)	100.6470(10)	90	90
V (Å^3)	1005.82(4)	2466.4(3)	5519.2(7)
Z	2	4	8
D_{calcd} (g·cm^{-3})	1.385	1.599	1.454
Crystal size (mm)	0.347 × 0.284 × 0.176	0.281 × 0.129 × 0.068	0.143 × 0.114 × 0.096
F(000)	436.0	1204.0	2480.0
Abs coeff (mm^{-1})	0.103	0.981	1.182
θ range (°)	4.658 to 52.774	4.858 to 52.76	5.158 to 52.756
Range *h*,*k*,*l*	−8/8, −11/11, −22/22	−17/17, −9/9, −30/30	−21/20, −17/17, −28/28
No. total refl.	25053	44081	98249
No. unique refl.	4116	5041	5616
Comp. θ_{max} (%)	99	100	99.4
Max/min transmission	0.982/0.966	0.981/0.765	0.619/0.745
Data/restraints/parameters	4116/0/270	5041/12/326	5616/0/326
Final *R* [$I > 2\sigma(I)$]	R_1 = 0.0558; wR_2 = 0.1550	R_1 = 0.0584; *w*R_2 = 0.1487	R_1 = 0.1190; wR_2 = 0.2982
R indices (all data)	R_1 = 0.0735; wR_2 = 0.1751	R_1 = 0.0852; wR_2 = 0.1653	R_1 = 0.1473; wR_2 = 0.3191
Goodness of fit / F^2	1.047	1.083	1.170
Largest diff. peak/hole (eÅ^{-3})	0.38/−0.32	0.56/−0.78	1.42/−0.97

CIF files have been deposited at the Cambridge Crystallographic Data Center and were allocated the deposition numbers CCDC 1580128 for **2**, 1580129 for **3**, and 1580130 for **5**. These data can be obtained free of charge via http://www.ccdc.cam.ac.uk/conts/retrieving.html (or from the Cambridge Crystallographic Data Centre, 12, Union Road, Cambridge CB2 1EZ, UK; fax: +44 1223 336033).

3.2. Synthetic Procedures

3.2.1. [(4-F–C_6H_4)C(O)CH=C(CH_3)N(H)-*o*-C_6H_4N=CH–(2-OH,5-NO_2–C_6H_3)] (**2**)

Half-unit **1** (200 mg, 0.740 mmol) was dissolved in MeOH (10 mL). Then, 160.8 mg (0.962 mmol) of 5-nitrosalicylaldehyde, previously dissolved in MeOH (10 mL), was added. The reaction mixture was stirred at room temperature for 6 h, leading to the formation of a yellow-mustard solid. The resulting suspension was filtered, washed three times with 5 mL of cold (−30 °C) MeOH and three time more with 5 mL of diethyl ether, and dried in vacuo, affording 247.3 mg (79.7% yield) of a yellow-mustard powder. Recrystallization by slow evaporation of a saturated dichloromethane solution deposited orange single crystals suitable for X-ray structure determination. mp 164–166 °C (Dec). Anal. calcd for $C_{23}H_{18}FN_3O_4$ (419.41 g·mol^{-1}): C, 65.87; H, 4.33; N, 10.02; found: C, 65.43; H, 4.01; N, 9.46. HRMS–ESI$^+$ (based on $C_{23}H_{18}N_3O_4FNa$) *m*/*z* calcd: 442.1174; found: 442.1177 [M + Na]$^+$. FT-IR (KBr pellet, cm^{-1}): 3441(w) ν(O–H), 3070(w) ν(N–H), 2995(vw), 2916(vw) ν(C–H aryl) 2848(vw) ν(C–H alkyl), 1614(w), 1584(s) ν(C⋯N), ν(C⋯O) and/or ν(C⋯C), 1479(s), 1338(s) $\nu_{asym}(NO_2)$, $\nu_{sym}(NO_2)$, 1296(s) ν(C–F). ^{1}H NMR (400 MHz, CD_2Cl_2): 13.71 (s, 1 H, O–*H*), 13.05 (br s, 1 H, N–*H*), 8.79 (s, 1 H, N=C*H*), 8.41 (d, 1 H, *J* = 4.0 Hz, *o*-C_6H_4), 8.20 (dd, 1 H, *J* = 12.0 Hz, 4.0 Hz, C_6H_3), 7.92 (dd, 2 H, *J* =8.0 Hz, 4.0 Hz, *p*-C_6H_4), 7.37 (m, 4 H, *o*-C_6H_4 + C_6H_3), 7.29 (dd, *J* = 8.0 Hz, 4.0 Hz, 1 H, *o*-C_6H_4), 7.11 (t, *J* = 8.0 Hz, 2 H, C_6H_4F), 7.02 (d, *J* = 12.0 Hz, 1 H, *o*-C_6H_4), 5.94 (s, 1 H, CH=C), 2.09 (s, 3 H, CH_3). ^{13}C NMR (100 MHz, CD_2Cl_2): 187.8 (*C*=O), 166.9 (*C*–OH), 165.1 (d, $J_{C,F}$ = 252 Hz, *C*–F), 162.9 (CH=*C*), 162.4 (N=CH), 143.0 (C–NO_2), 140.6 (C–N=), 136.6 (C–NH), 133.9 (C_{quat}, C_6H_4F), 129.7 (d, $J_{C,F}$ = 9 Hz, *CH*, C_6H_4F), 129.0 (*C*H, *o*-C_6H_4), 128.8 (*C*H, *o*-C_6H_4), 128.7 (*C*H, *o*-C_6H_4), 127.8 (*C*H, C_6H_3), 127.3 (*C*H, C_6H_3), 119.4 (*C*H, C_6H_3), 119.0 (C_{quat}, C_6H_3–CH=N), 118.6 (*C*H, *o*-C_6H_4),115.4 (d, $J_{C,F}$ = 21 Hz, *C*H, C_6H_4F), 94.6 (*C*H=C), 20.5 (*C*H_3). ^{19}F NMR (376 MHz, CD_2Cl_2): −110.15 (s, C*F*).

3.2.2. [{(4-F–C_6H_4)C(O)CH=C(CH_3)N-*o*-C_6H_4N=CH–(2-O,5-NO_2–C_6H_3)}FeCl] (**3**)

A Schlenk tube containing a magnetic stirring bar was charged with 300 mg (0.715 mmol) of proligand **2**, and placed in vacuo for 30 min. Then the solid was dissolved in 10 mL of freshly distilled THF. The resulting solution was stirred and 161 mg (1.431 mmol) of potassium *tert*-butoxide was added, generating an orange solid in the mixture that was stirred for an additional 30 min. Then 174 mg (1.073 mmol) of anhydrous $FeCl_3$, dissolved in 10 mL of freshly distilled THF, was added to the reaction mixture that turned dark brown. Stirring was continued for 4 h at room temperature, a dark solid appeared after 1 h. The solvent was completely evaporated in vacuo. The solid residue was extracted with 20 mL of dichloromethane. The resulting solution was filtered, and concentrated to obtain a dark brown solid which was filtered off and dried in vacuo for 2 h, affording 314 mg (86.4% yield) of microcrystalline dark brown solid. Recrystallization by slow evaporation of a saturated dichloromethane solution deposited black single crystals suitable for X-ray structure determination. mp 250–252 °C (dec). Anal. calcd for $C_{23}H_{16}ClFFeN_3O_4$ (508.69 g·mol^{-1}): C, 54.31; H, 3.17; N, 8.26; found: C, 54.53; H, 3.29; N, 8.04. HRMS-ESI$^+$ (based on $C_{23}H_{16}N_3O_4F^{35}ClNa^{56}Fe$) *m*/*z* calcd: 531.0055; found: 531.0056 [M + Na]$^+$. FT-IR (KBr pellet, cm^{-1}): 3229(w) ν(O–H), 3064(v) ν(C–H aryl), 2964(w), 2922(w) ν(C–H alkyl), 1608(s), 1599(w), 1548(s) ν(C⋯N), ν(C⋯O) and/or ν(C⋯C), 1492(s) ν_{asym} (NO_2), 1320(s), $\nu_{sym}(NO_2)$, 1102 (m) ν(C–F).

3.2.3. [{(η^5-C_5H_5)Fe(η^5-C_5H_4)C(O)CH=C(CH_3)N-o-C_6H_4N=CH–(2-O,5-OCH_3–C_6H_3)}FeCl] (**5**)

A Schlenk tube containing a magnetic stirring bar was charged with 300 mg (0.833 mmol) of the organometallic half-unit **4** and placed under vacuum for 30 min. Freshly distilled THF (10 mL)

and 103.9 μL (0.833 mmol) of 5-methoxysalicylaldehyde were successively added. The resulting dark orange solution was stirred for 15 min before adding 186.9 mg (1.666 mmol) of potassium *tert*-butoxide. The reaction mixture was stirred for an additional 15 min leading to the formation of a light orange suspension. Addition of 207.2 mg (1.245 mmol) of anhydrous $FeCl_3$, dissolved in 15 mL of freshly distilled THF, generated a dark-brown slurry. Work up as above for **4** provided a dark solid that was filtered off and adsorbed on a column packed with silica gel. Elution with CH_3Cl/MeOH mixture (10:1) produced the release of a dark-brown band that was collected. The solvents were evaporated in vacuo, and the solid material was recrystallized by slow diffusion of diethyl ether into a saturated acetonitrile solution of the compound, affording 384.6 mg (79.1% yield) of black needles suitable for X-ray structure determination. mp 280–282 °C. Anal. calcd for $C_{28}H_{24}ClFe_2N_2O_3$ (583.65 g·mol^{-1}): C, 57.62; H, 4.14; N, 4.80; found: C, 57.46; H, 4.37; N, 4.96. HRMS-ESI$^+$ (based on $C_{28}H_{24}N_2O_3{}^{35}ClNa^{56}Fe_2$) m/z calcd: 606.00664; found: 606.0065 [M + Na]$^+$. FT-IR (KBr pellet, cm^{-1}): 3432(m), ν(O–H); 3064(w), 3004(w), 2948(w) ν(C–H aryl), 2924(w), 2850(vw), 2834(m) ν(C–H alkyl), 1602(s), 1552(s), 1536(s) ν(C⋯N), ν(C⋯O) and/or ν(C⋯C), 1362(vs), 1266(s), 1324(m) ν(C–O).

4. Conclusions

Two new pentacoordinated chloro-iron(III) complexes of unsymmetrically substituted $[N_2O_2]^{2-}$ tetradentate Schiff-base ligands bearing either a pair of donor or acceptor substituents along with the Schiff-base proligand possessing the electron-withdrawing fluorine and nitro groups have been prepared and fully characterized. In the two D-π-D′ and A-π-A′ compounds, the two donor or acceptor units are connected through the conjugated iron(III)-centered macroacyclic Schiff-base core. The two complexes exhibited solvatochromic behavior that is suggestive of potential NLO activity. Although the nature of the substituents (acceptor vs. donor) does not have significant influence on the values of absorption maxima, electron-withdrawing and electron-donating substituents produce anodic and cathodic shifts, respectively, in both Schiff-base-ligand-based Fe(III) complexes, specifically in Fe(III)/Fe(II) redox potential values. Single-crystal X-ray diffraction analyses showed that the iron(III) ion adopts a strongly distorted square-pyramidal geometry. Moreover, the iron-to-imine bond lengths, close to 2.10 Å, put both complexes in the high-spin state. This finding was further confirmed by solid-phase magnetic measurements. Furthermore, a synthetic strategy utilizing the lability of the chloro ligand is anticipated to open up avenues for accessing a vast array of new mixed-ligand iron(III) complexes.

Supplementary Materials: The following are available online at www.mdpi.com/2304-6740/6/1/5/s1. Cif and cif-checked files. Figure S1: Packing diagram of **2** showing the hydrogen bonding interactions, Figure S2: Packing diagram of **3**·CH_2Cl_2 showing the hydrogen bonding interactions implying the dichloromethane crystallization molecules, Figure S3: Experimental UV-vis spectra of complexes **3** (top, full line) and **5** (bottom, full line) recorded in DMSO at 20 °C, and their respective deconvoluted spectra (dotted lines), Table S1: Selected bond distances (Å) and angles (°) for compounds **3**·CH_2Cl_2, Table S2: Selected bond distances (Å) and angles (°) for compound **5**·0.5MeCN, Table S3: Atomic occupancy for complex **5**, Table S4: Hydrogen bond interaction parameters for proligand **2**.

Acknowledgments: Financial support from the Fondo Nacional de Desarrollo Científico y Tecnológico [FONDECYT (Chile), grant no. 1130105 (David Carrillo, Carolina Manzur and Mauricio Fuentealba), the Vicerrectoría de Investigación y Estudios Avanzados, Pontificia Universidad Católica de Valparaíso, Chile (David Carrillo, Carolina Manzur and Mauricio Fuentealba), the CNRS and the Université de Rennes 1 is gratefully acknowledged. This research has been performed as part of the Chilean-French International Associated Laboratory "Multifunctional Molecules and Materials" (LIA M3-CNRS N° 1027). The authors are grateful to O. Cador (ISCR, Rennes), F. Lambert and P. Jehan (CRMPO, Rennes) for helpful assistance with magnetic measurements and HRMS, respectively. Jonathan Cisterna thanks the CONICYT (Chile) for support of a graduate fellowship.

Author Contributions: David Carrillo and Carolina Manzur conceived and designed the experiments; Jonathan Cisterna performed the experiments; Mauricio Fuentealba, Jean-René Hamon, Carolina Manzur and David Carrillo analyzed the data; Vania Artigas and Mauricio Fuentealba performed the crystallographic studies, Paul Hamon carried out the NMR experiments; Jean-René Hamon wrote the paper, and Jonathan Cisterna, Carolina Manzur and David Carrillo participated to the article editing.

Conflicts of Interest: The authors declare no conflict of interest.

References

1. Schiff, H. Mittheilungen aus dem universitätslaboratorium in pisa: Eine neue reihe organischer basen. *Justus Liebigs Ann. Chem.* **1864**, *131*, 118–119. [CrossRef]
2. Hobday, M.D.; Smith, T.D. *N,N'*-ethylenebis(salicylideneiminato) transition metal ion chelates. *Coord. Chem. Rev.* **1973**, *9*, 311–337. [CrossRef]
3. Garnovskii, A.D.; Nivorozhkin, A.L.; Minkin, V.I. Ligand environment and the structure of Schiff base adducts and tetracoordinated metal-chelates. *Coord. Chem. Rev.* **1993**, *126*, 1–69. [CrossRef]
4. Vigato, P.A.; Tamburini, S. Advances in acyclic compartmental ligands and related complexes. *Coord. Chem. Rev.* **2008**, *252*, 1871–1995. [CrossRef]
5. Yang, J.; Shi, R.; Zhou, P.; Qiu, Q.; Li, H. Asymmetric Schiff bases derived from diaminomaleonitrile and their metal complexes. *J. Mol. Struct.* **2016**, *1106*, 242–258. [CrossRef]
6. Pfeiffer, P.; Breith, E.; Lubbe, E.; Tsumaki, T. Tricyclische orthokondensierte nebenvalenzringe. *Justus Liebigs Ann. Chem.* **1933**, *503*, 84–130. [CrossRef]
7. Costes, J.-P.; Cros, G.; Darbieu, M.H.; Laurent, J.-P. The non-template synthesis of novel non-symmetrical, tetradentate Schiff bases. Their nickel(II) and cobalt(III) complexes. *Inorg. Chim. Acta* **1982**, *60*, 111–114. [CrossRef]
8. Guerriero, P.; Tarnburini, S.; Vigato, P.A. From mononuclear to polynuclear macrocyclic or macroacyclic complexes. *Coord. Chem. Rev.* **1995**, *139*, 17–243. [CrossRef]
9. Clarke, R.M.; Storr, T. The chemistry and applications of multimetallic salen complexes. *Dalton Trans.* **2014**, *43*, 9380–9391. [CrossRef] [PubMed]
10. Menati, S.; Amiri Rudbari, H.; Askari, B.; Riahi Farsani, M.; Jalilian, F.; Dini, G. Synthesis and characterization of insoluble cobalt(II), nickel(II), zinc(II) and palladium(II) Schiff base complexes: Heterogeneous catalysts for oxidation of sulfides with hydrogen peroxide. *C. R. Chimie* **2016**, *19*, 347–356. [CrossRef]
11. Drozdzak, R.; Allaert, B.; Ledoux, N.; Dragutan, I.; Dragutan, V.; Verpoort, F. Ruthenium complexes bearing bidentate Schiff base ligands as efficient catalysts for organic and polymer syntheses. *Coord. Chem. Rev.* **2005**, *249*, 3055–3074. [CrossRef]
12. Wezenberg, S.J.; Kleij, A.W. Material Applications for Salen Frameworks. *Angew. Chem. Int. Ed.* **2008**, *47*, 2354–2364. [CrossRef] [PubMed]
13. Castillo-Martinez, E.; Carretero-Gonzalez, J.; Armand, M. Polymeric Schiff bases as low-voltage redox centers for sodium-ion batteries. *Angew. Chem. Int. Ed.* **2014**, *53*, 5341–5345. [CrossRef] [PubMed]
14. Di Bella, S. Second-order nonlinear optical properties of transition metal complexes. *Chem. Soc. Rev.* **2001**, *30*, 355–366. [CrossRef]
15. Righetto, S.; Di Bella, S. Synthesis, characterization, optical absorption/fluorescence spectroscopy, and second-order nonlinear optical properties of aggregate molecular architectures of unsymmetrical Schiff-base zinc(II) complexes. *Dalton Trans.* **2014**, *43*, 2168–2175. [CrossRef]
16. Kaim, W.; Schwederski, B. Bioinorganic chemistry: Inorganic elements. In *The Chemistry of Life*; John Wiley & Sons: Chichester, UK, 1994; ISBN 0-471-94369-X.
17. Weber, B.; Jäger, E.-G. Structure and magnetic properties of iron(II/III) complexes with $N_2O_2^{2-}$ coordinating Schiff base like ligands. *Eur. J. Inorg. Chem.* **2009**, 465–477. [CrossRef]
18. Domracheva, N.; Pyataev, A.; Manapov, R.; Gruzdev, M.; Chervonova, U.; Kolker, A. Structural, magnetic and dynamic characterization of liquid crystalline iron(III) Schiff base complexes with asymmetric ligands. *Eur. J. Inorg. Chem.* **2011**, 1219–1229. [CrossRef]
19. Phonsri, W.; Martinez, V.; Davies, C.G.; Jameson, G.N.L.; Moubaraki, B.; Murray, K.S. Ligand effects in a heteroleptic bis-tridentate iron(III) spin crossover complex showing a very high $T_{1/2}$ value. *Chem. Commun.* **2016**, *52*, 1443–1446. [CrossRef] [PubMed]
20. Krüger, C.; Augustín, P.; Nemec, I.; Trávnícek, Z.; Oshio, H.; Boca, R.; Renz, F. Spin crossover in iron(III) complexes with pentadentate Schiff base ligands and pseudohalido coligands. *Eur. J. Inorg. Chem.* **2013**, 902–915. [CrossRef]

21. Kruger, C.; Augustin, P.; Dlhan, L.; Pavlik, J.; Moncol, J.; Nemec, I.; Boca, R.; Renz, F. Iron(III) complexes with pentadentate Schiff-base ligands: Influence of crystal packing change and pseudohalido coligand variations on spincrossover. *Polyhedron* **2015**, *87*, 194–201. [CrossRef]
22. Matsumoto, N.; Kimoto, K.; Ohyoshi, A.; Maeda, Y. Synthesis and characterization of iron(III) complexes with unsymmetrical quadridentate Schiff bases, and spin equilibrium behavior in solution. *Bull. Chem. Soc. Jpn.* **1984**, *57*, 3307–3311. [CrossRef]
23. Fitzsimmons, B.W.; Smith, A.W.; Larkworthy, L.F.; Rogers, K.A. Transition metal–Schiff base complexes. Part VI. Mössbauer and magnetic investigations of some iron(II) and iron(III) systems. *J. Chem. Soc. Dalton Trans.* **1973**, 676–680. [CrossRef]
24. Shyu, H.-L.; Wei, H.-H.; Lee, G.-H.; Wang, Y. Structure, magnetic properties and epoxidation activity of iron(III) salicylaldimine complexes. *J. Chem. Soc. Dalton Trans.* **2000**, 915–918. [CrossRef]
25. Gerloch, M.; Mabbs, F.E. The crystal and molecular structure of chloro-(*NN*′-bis-salicylidene-ethylenediamine)iron(III) as a hexaco-ordinate Dimer. *J. Chem. Soc. A* **1967**, 1900–1908. [CrossRef]
26. Chiang, W.; Thompson, M.E.; Van Engen, D. Synthesis and Nonlinear Optical Properties of Inorganic Coordination Polymers. *Spec. Publ. R. Soc. Chem.* **1991**, *91*, 210–216.
27. Elmali, A.; Karakas, A.; Unver, H. Nonlinear optical properties of bis[(p-bromophenyl-salicylaldiminato) chloro]iron(III) and its ligand *N*-(4-bromo)-salicylaldimine. *Chem. Phys.* **2005**, *309*, 251–257. [CrossRef]
28. Karuppasamy, P.; Thiruppathi, D.; Vijaya Sundar, J.; Rajapandian, V.; Ganesan, M.; Rajendran, T.; Rajagopal, S.; Nagarajan, N.; Rajendran, P.; Sivasubramanian, V.K. Spectral, computational, electrochemical and antibacterial studies of iron(III)-salen complexes. *Arab. J. Sci. Eng.* **2015**, *40*, 2945–2958. [CrossRef]
29. Cisterna, J.; Artigas, V.; Fuentealba, M.; Hamon, P.; Manzur, C.; Dorcet, V.; Hamon, J.-R.; Carrillo, D. Nickel(II) and copper(II) complexes of new unsymmetrically-substituted tetradentate Schiff base ligands: Spectral, structural, electrochemical and computational studies. *Inorg. Chim. Acta* **2017**, *462*, 266–280. [CrossRef]
30. Silvestri, A.; Barone, G.; Ruisi, G.; Lo Giudice, M.T.; Tumminello, S. The interaction of native DNA with iron(III)-*N*,*N*′-ethylene-bis(salicylideneiminato)-chloride. *J. Inorg. Biochem.* **2004**, *98*, 589–594. [CrossRef] [PubMed]
31. Darensbourg, D.J.; Ortiz, C.G.; Billodeaux, D.R. Synthesis and structural characterization of iron(III) salen complexes possessing appended anionic oxygen donor ligands. *Inorg. Chim. Acta* **2004**, *357*, 2143–2149. [CrossRef]
32. Novoa, N.; Roisnel, T.; Hamon, P.; Kahlal, S.; Manzur, C.; Ngo, H.M.; Ledoux-Rak, I.; Saillard, J.-Y.; Carrillo, D.; Hamon, J.-R. Four-coordinate nickel(II) and copper(II) complex based ONO tridentate Schiff base ligands: Synthesis, molecular structure, electrochemical, linear and nonlinear properties, and computational study. *Dalton Trans.* **2015**, *44*, 18019–18037. [CrossRef] [PubMed]
33. Fuentealba, M.; Trujillo, A.; Hamon, J.-R.; Carrillo, D.; Manzur, C. Synthesis, characterization and crystal structure of the tridentate metalloligand formed from mono-condensation of ferrocenoylacetone and 1,2-phenylenediamine. *J. Mol. Struct.* **2008**, *881*, 76–82. [CrossRef]
34. Trujillo, A.; Fuentealba, M.; Carrillo, D.; Manzur, C.; Ledoux-Rak, I.; Hamon, J.-R.; Saillard, J.-Y. Synthesis, spectral, structural, second-order nonlinear optical properties and theoretical studies On new organometallic donor-acceptor substituted nickel(II) and copper(II) unsymmetrical Schiff-base complexes. *Inorg. Chem.* **2010**, *49*, 2750–2764. [CrossRef] [PubMed]
35. Celedón, S.; Fuentealba, M.; Roisnel, T.; Ledoux-Rak, I.; Hamon, J.-R.; Carrillo, D.; Manzur, C. Side-chain metallopolymers containing second-order NLO-active bimetallic NiII and PdII Schiff-base complexes: Syntheses, structures, electrochemical and computational studies. *Eur. J. Inorg. Chem.* **2016**, 3012–3023. [CrossRef]
36. Cisterna, J.; Dorcet, V.; Manzur, C.; Ledoux-Rak, I.; Hamon, J.R.; Carrillo, D. Synthesis, spectral, electrochemical, crystal structures and nonlinear optical properties of unsymmetrical Ni(II) and Cu(II) Schiff base complexes. *Inorg. Chim. Acta* **2015**, *430*, 82–90. [CrossRef]
37. Mahmoud, W.H.; Mahmoud, N.F.; Mohamed, G.G. Mixed ligand complexes of the novel nanoferrocene based Schiff base ligand (HL): Synthesis, spectroscopic characterization, MOE studies and antimicrobial/anticancer activities. *J. Organomet. Chem.* **2017**, *848*, 288–301. [CrossRef]

38. Ouennoughi, Y.; Eddine Karce, H.; Aggoun, D.; Lanez, T.; Ruiz-Rosas, R.; Bouzerafa, B.; Ourari, A.; Morallon, E. A novel ferrocenic copper(II) complex salen-like, derived from 5-chloromethyl-2-hydroxyacetophenone and *N*-ferrocenmethylaniline: Design, spectral approach and solvent effect towards electrochemical behavior of Fc^+/Fc redox couple. *J. Organomet. Chem.* **2017**, *848*, 344–351. [CrossRef]
39. Sharif, S.; Denisov, G.S.; Toney, M.D.; Limbach, H.-H. NMR studies of solvent-assisted proton transfer in a biologically relevant Schiff base: Toward a distinction of geometric and equilibrium H-bond isotope effects. *J. Am. Chem. Soc.* **2006**, *128*, 3375–3387. [CrossRef] [PubMed]
40. Dziembowska, T.; Szafran, M.; Katrusiak, A.; Rozwadowski, Z. Crystal structure of and solvent effect on tautomeric equilibrium in Schiff base derived from 2-hydroxy-1-naphthaldehyde and methylamine studied by X-ray diffraction, DFT, NMR and IR methods. *J. Mol. Struct.* **2009**, *929*, 32–42. [CrossRef]
41. Dunitz, J.D.; Orgel, L.E.; Rich, A. The crystal structure of ferrocene. *Acta Crystallogr.* **1956**, *9*, 373–375. [CrossRef]
42. Gilli, P.; Bertolasi, V.; Ferretti, V.; Gilli, G. Evidence for intramolecular N–H···O resonance-assisted hydrogen bonding in β-enaminones and related heterodienes. A combined crystal-structural, IR and NMR spectroscopic, and quantum-mechanical investigation. *J. Am. Chem. Soc.* **2000**, *122*, 10405–10417. [CrossRef]
43. Addison, A.W.; Nageswara, T.; Reedijk, J.; van Rijn, J.; Verchoor, G.C. Synthesis, structure, and spectroscopic properties of copper(II) compounds containing nitrogen-sulphur donor ligands ; the crystal and molecular structure of aqua[1,7-bis(*N*-methylbenzimidazol-2′-yl)-2,6-dithiaheptane]copper(II) perchlorate. *J. Chem. Soc. Dalton Trans.* **1984**, 1349–1356. [CrossRef]
44. Gerloch, M.; Mabbs, F.E. The crystal and molecular structure of *NN*′-bis(salicylideneiminato)-iron(III)chloride as a five-co-ordinate monomer. *J. Chem. Soc. A* **1967**, 1598–1608. [CrossRef]
45. Elmali, A.; Elerman, Y.; Svoboda, I.; Fuess, H. Structure of [*N*,*N*′-*o*-Phenylenebis-(salicylideneaminato)] iron(III) chloride as a five-coordinate monomer. *Acta Crystallogr.* **1993**, *C49*, 1365–1367. [CrossRef]
46. Elerman, Y.; Kabak, M.; Tllko, D. A Five-coordinated monomer of chloro-[*N*,*N*′-(di-2-hydroxy-1-naphthylidene)-1,2-diaminobenzene]iron(III). *Acta Crystallogr.* **1997**, *C53*, 712–714. [CrossRef]
47. Elmali, A.; Kavlakoglu, E.; Elerman, Y.; Svoboda, I. A complex containing both five- and six-coordinate [bis(5-bromosalicylidene)benzene-1,2-diimine]chloro-iron(III). *Acta Crystallogr.* **2000**, *C56*, 1097–1099. [CrossRef]
48. Oyaizu, K.; Tsuchida, E. Crystal structure and reactivity of a five-coordinate chloroiron(III) complex with a bulky tetradentate Schiff base ligand. *Inorg. Chim. Acta* **2003**, *355*, 414–419. [CrossRef]
49. Dyers, L., Jr.; Que, S.Y.; VanDerveer, D.; Bu, X.R. Synthesis and structures of new salen complexes with bulky groups. *Inorg. Chim. Acta* **2006**, *359*, 197–203. [CrossRef]
50. Calligaris, M.; Nardin, G.; Randaccio, L. Structural aspects of metal complexes with some tetradentate schiff bases. *Coord. Chem. Rev.* **1972**, *7*, 385–403. [CrossRef]
51. Oyaizu, K.; Dewi, E.L.; Tsuchida, E. A μ-oxo diiron(III) complex with a short Fe–Fe distance: Crystal structure of (μ-oxo)bis[*N*,*N*′-*o*-phenylenebis(salicylideneiminato)iron(III)]. *Inorg. Chim. Acta* **2001**, *321*, 205–208. [CrossRef]
52. Carré, B.; Costes, J.-P.; Tommasino, J.-B.; De Montauzon, D.; Soulet, F.; Fabre, P.-L. Electrochemical studies of Iron(III) Schiff base complexes—I. The monomeric FeIII(N_2O_2)Cl complexes. *Polyhedron* **1993**, *12*, 641–649. [CrossRef]
53. Armarego, W.L.F.; Chai, C.L.L. *Purification of Laboratory Chemicals*, 5th ed.; Butterworth-Heinemann, Elsevier Inc.: Amsterdam, The Netherlands, 2003; ISBN 978-0-7506-7571-0.
54. Kahn, O. *Molecular Magnetism*; VCH Publishers: New York, USA, 1993; ISBN 978-0471188384.
55. Dolomanov, O.V.; Bourhis, L.J.; Gildea, R.J.; Howard, J.A.K.; Puschmann, H. OLEX2: A complete structure solution, refinement and analysis program. *J. Appl. Crystallogr.* **2009**, *42*, 339–341. [CrossRef]
56. Sheldrick, G.M. Crystal structure refinement with *SHELXL*. *Acta Crystallogr.* **2015**, *C71*, 3–8. [CrossRef]
57. Sheldrick, G.M. A short history of *SHELX*. *Acta Crystallogr.* **2008**, *A64*, 112–122. [CrossRef] [PubMed]